Deep Learning-based Kinetic Analysis in Paper-based Analytical Cartridges Integrated with Field-effect Transistors

Hyun-June Jang[1,2]‡, Hyou-Arm Joung[3]‡, Artem Goncharov[3], Anastasia Gant Kanegusuku[4], Clarence W. Chan[5], Kiang-Teck Jerry Yeo[5,6], Wen Zhuang[1,2], Aydogan Ozcan[3,7,8,9*], Junhong Chen[1,2*]

[1]Pritzker School of Molecular Engineering, University of Chicago, Chicago, IL 60637, USA

[2]Chemical Sciences and Engineering Division, Physical Sciences and Engineering Directorate, Argonne National Laboratory, Lemont, IL 60439, USA

[3]Department of Electrical and Computer Engineering, University of California, Los Angeles, CA 90095, USA

[4]Department of Pathology and Laboratory Medicine, Loyola University Medical Center, Maywood, IL 60153

[5]Department of Pathology, The University of Chicago, Chicago, IL 60637, USA

[6]Pritzker School of Medicine, The University of Chicago, Chicago, IL 60637, USA

[7]Department of Bioengineering, University of California, Los Angeles, CA 90095, USA

[8]California NanoSystems Institute (CNSI), University of California, Los Angeles, CA 90095, USA

[9]Department of Surgery, David Geffen School of Medicine, University of California, Los Angeles, CA 90095, USA

‡These authors contributed equally to this work

*Correspondence: ozcan@ucla.edu, junhongchen@uchicago.edu

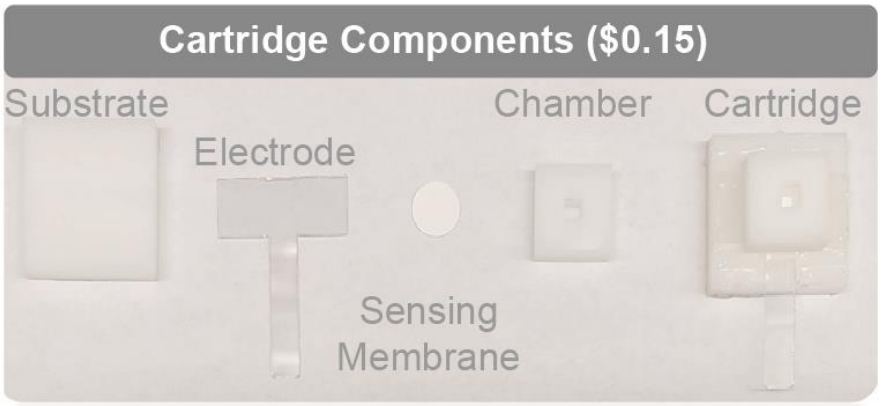

Types	Name	Cost/test (¢)
Materials	Acrylic Sheet	0.64
	Membrane	1.1
	Double-sided tape	4.1
	ITO electrode	3.8
Enzymes	Cholesterol esterase	1.8
	Cholesterol oxidase	1.2
	Peroxidase	1.5
Others (PBS, Tween20, TX-100)		<1
	Total cost/test	**14.56**

Table S1. Breaking down of material cost of cartridge components per test.

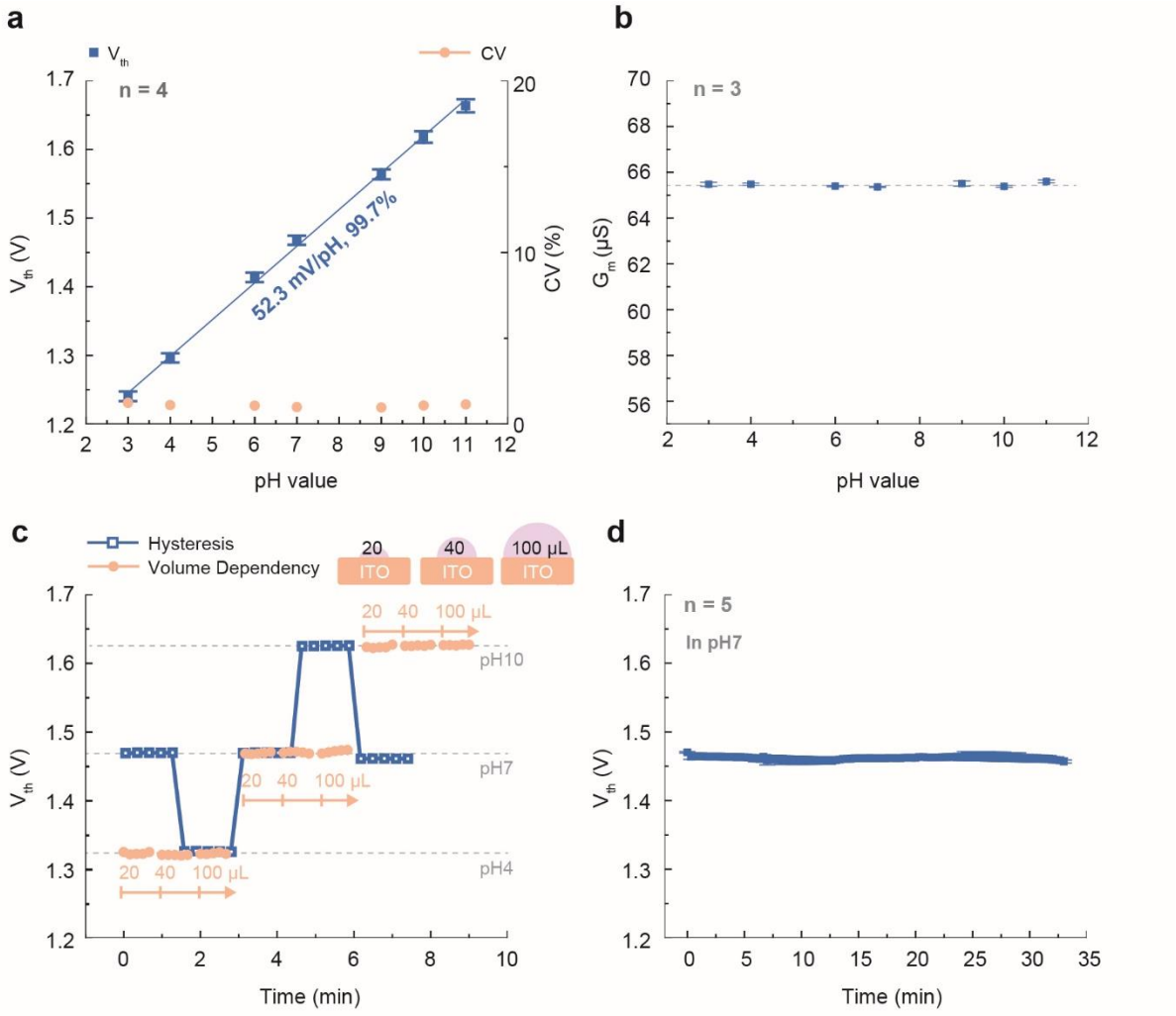

Figure S1. (a) V_{th} response to pH on the ITO surface over 4 different ITO tests and CV values of V_{th} for each pH. The pH sensitivity (calculated as the slope of pH versus V_{th}) was found to be 52.3 mV/pH. The device-to-device variation was negligible, with all CV values for V_{th} at each pH being no more than 1.3%. (b) G_m values as a function of pH variation on ITO. (c) Hysteresis was assessed by a rapid loop of pH changes (7-4-7-10-7), showing a reversible trend with changing pH values. The difference between the initial V_{th} value at the first pH 7 cycle and the final V_{th} value at the last pH 7 cycle was measured to be 8 mV. (d) Drift rate in pH 7 solution measured on five different ITO sensing electrodes was found to be 8 μV/min over 30 minutes.

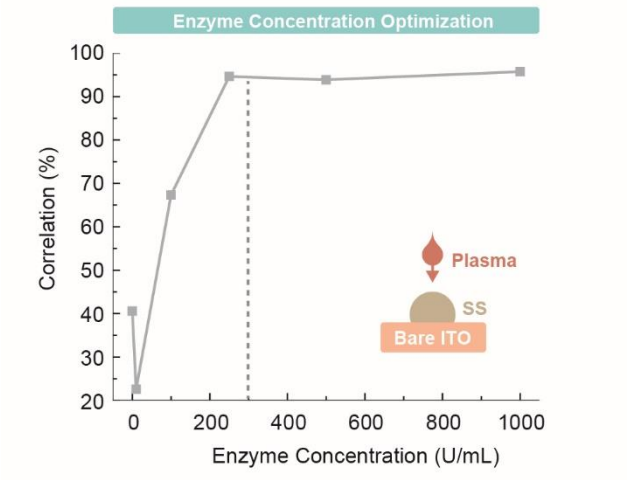

Figure S2. The correlation coefficient (r^2 value) was calculated for the range of cholesterol levels from 0 to 300 mg/dL in human plasma vs. enzyme concentrations of the sensing solution (SS). The SS is an enzyme solution including all detection components which is prepared for drying it on PSM. This experimental setup is based on wet chemistry approach (i.e., no cartridge, but solution phase). 19 uL SS was first placed on the bare ITO and sequentially 1 uL plasma samples were added on SS for tests. The cholesterol concentrations in plasma samples were measured using Roche Cobas instrumentation. Concentrations of enzymes exceeding 200 U/mL displayed saturated correlations (r^2 value), leading us to choose 300 U/mL enzyme concentrations for COE, COx, and POx in all subsequent experiments.

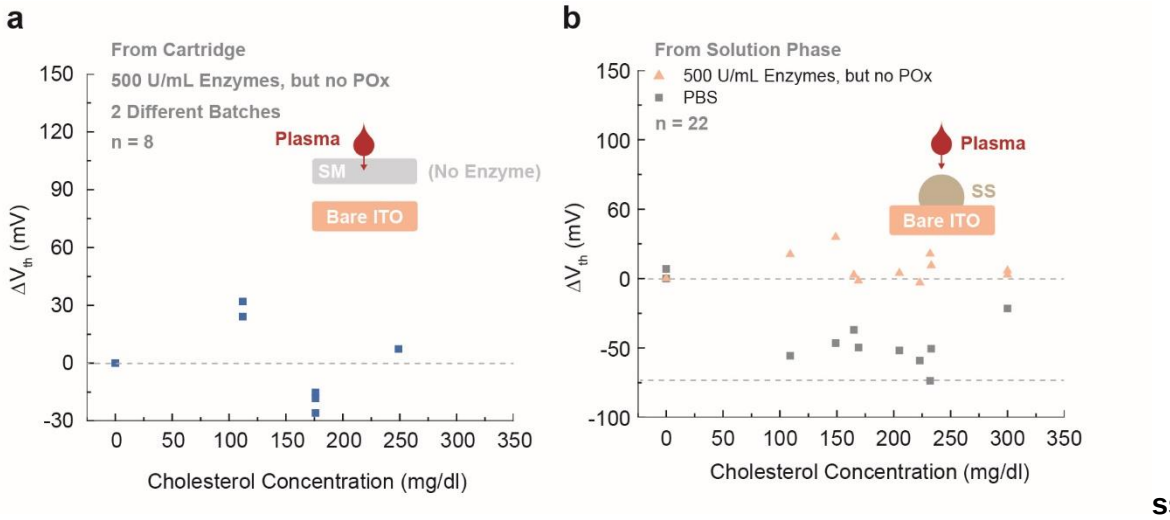

Figure S3. At a specific cholesterol concentration, the ΔV_{th} of human plasma relative to the V_{th} for lipoprotein-free plasma was measured. Without the POx enzyme, no correlating sensing signals were obtained for either the (a) dry or (b) wet chemistry approaches, indicating that POx played a critical role in generating electroactive enzymatic signals such as protons. For both the dry and wet chemistry approaches, 500 U/mL of COx and COE diluted in PBS were utilized. In the absence of enzyme addition (i.e., only the presence of PBS components in the sensing solution), negative levels of ΔV_{th} were observed across all human plasma samples due to non-specific binding signals of human plasma components and ITO (Figure S3b)."

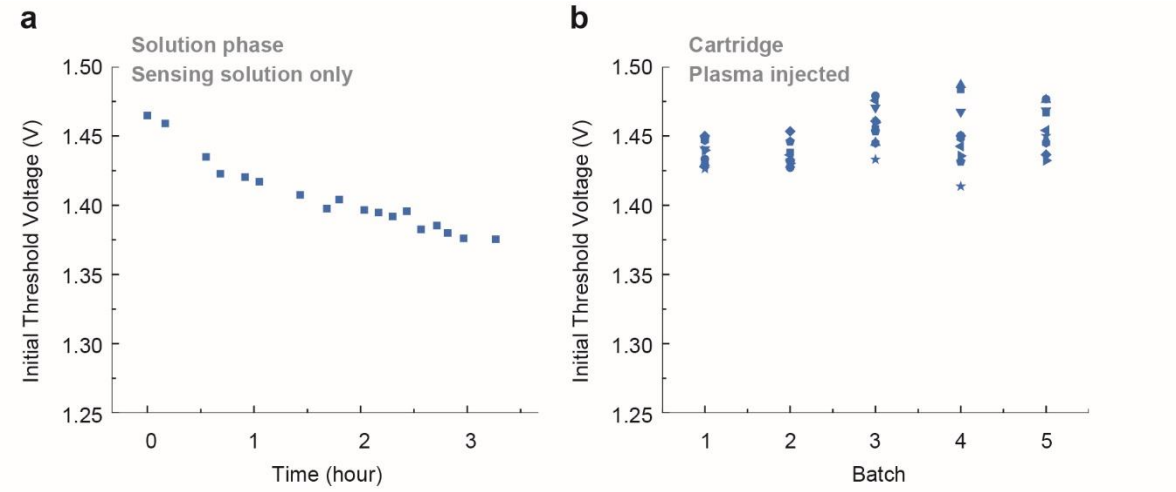

Figure S4. The initial V_{th} changes over time were observed in two scenarios: (a) SS itself without adding human plasma and (b) the cartridge obtained after injections of different random human plasma samples in the cartridge. The initial V_{th} of the cartridge was measured after fabrication from 2 hours to 6 days from each batch.

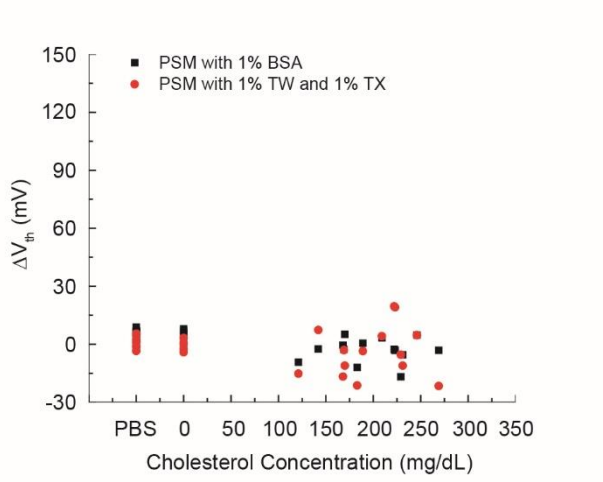

Figure S5. ΔV_{th} distribution of the cartridge without enzyme components, but dried with 1) 1% BSA and 2) 1% tween 20 and triton X-100 (surfactant only), was analyzed when adding 1) PBS buffer, 2) lipoprotein-free plasma, and 3) human plasma samples with specific cholesterol concentrations. A total of 16 cartridges were tested with PBS, with additional 16 tested with zero-cholesterol plasma and 28 tested with human plasma. A large dispersion of ΔV_{th} is shown from adding human plasma over the case of PBS and lipoprotein-free plasma due to sample matrix effects.

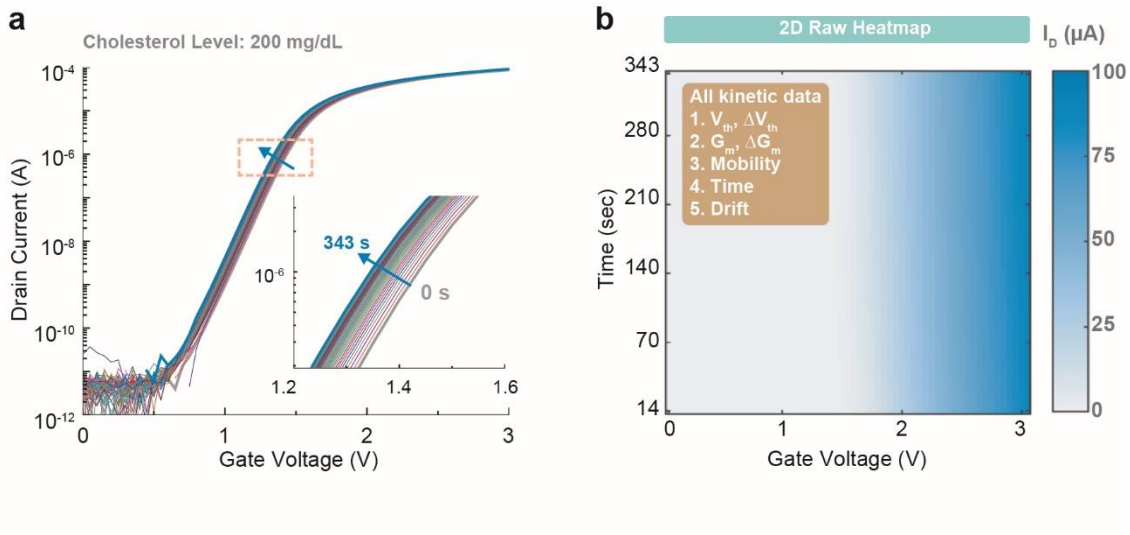

Figure S6. (a) Representative transfer curves captured over 343 sec (total 49 measurements) from 200 mg/dL plasma sample. (b) Transfer curves of Figure S6 (a) over time represented as a 2D current heatmap.

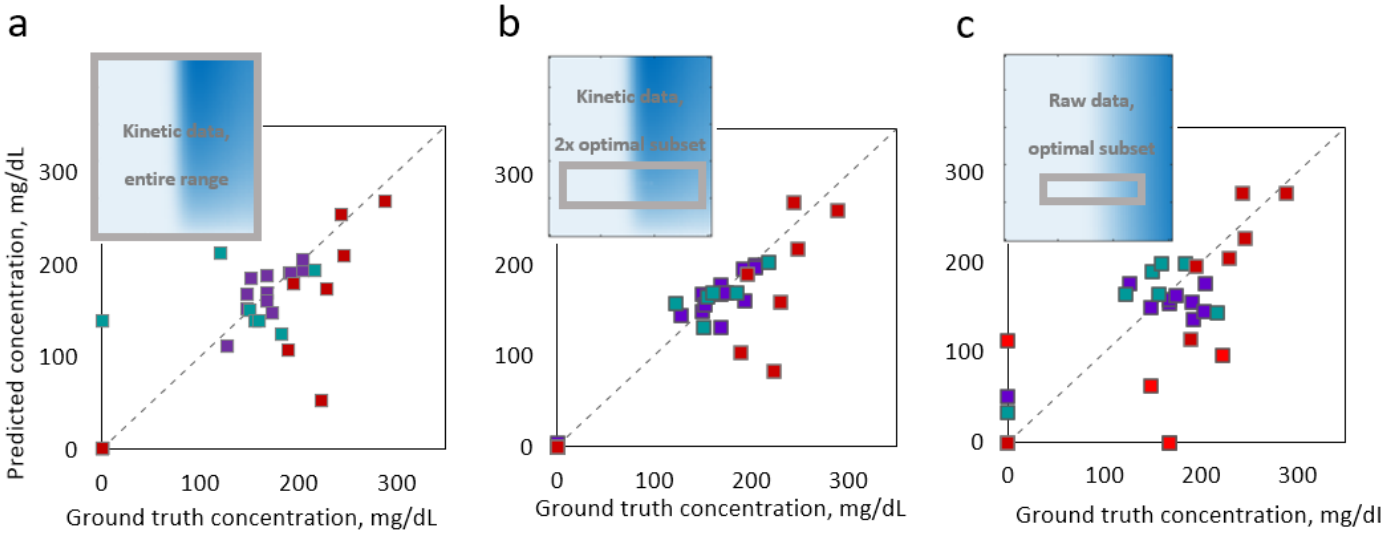

Model	Metric				
	R^2				CV, %
	Overall	Batch 1	Batch 2	Batch 3	
Optimal model	0.97	0.97	0.98	0.98	4.65
Entire range	0.75	0.64	0.96	0.47	21.9 %
2x more data	0.75	0.69	0.96	0.92	15.6
Raw data input	0.80	0.97	0.78	0.65	>20 %

Figure S7. Blind testing predictions for models with non-optimal input subsets. (a) Blind testing predictions for the model with the kinetic data from the entire operation range; (b) Blind testing predictions for the model with the kinetic data from the 2x optimal range; (c) Blind testing predictions for the model with the raw data from the optimal range. r^2 and CV summarized for deep learning models with different input data.

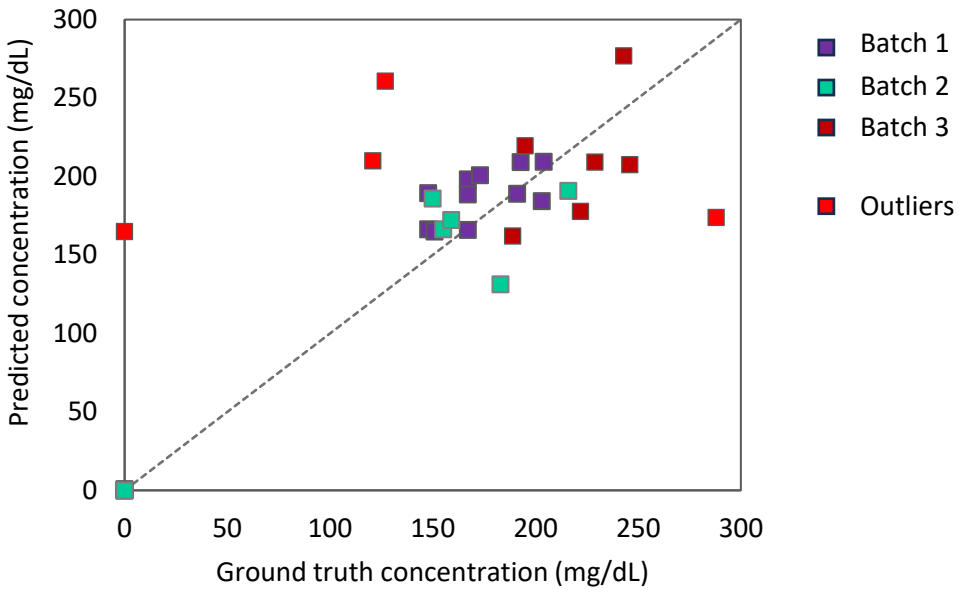

Figure S8. The predicted cholesterol concentration was determined using a single model trained on samples from all three batches, with an r^2 value of 0.886, excluding outliers. The CV for the overall range is 10.85%. Within specific ranges, the CV values for cholesterol concentrations of 100 to 150, 150 to 200, 200 to 240, and > 240 mg/dL are 10.95%, 8.03%, 10.26%, and 20.21%, respectively.

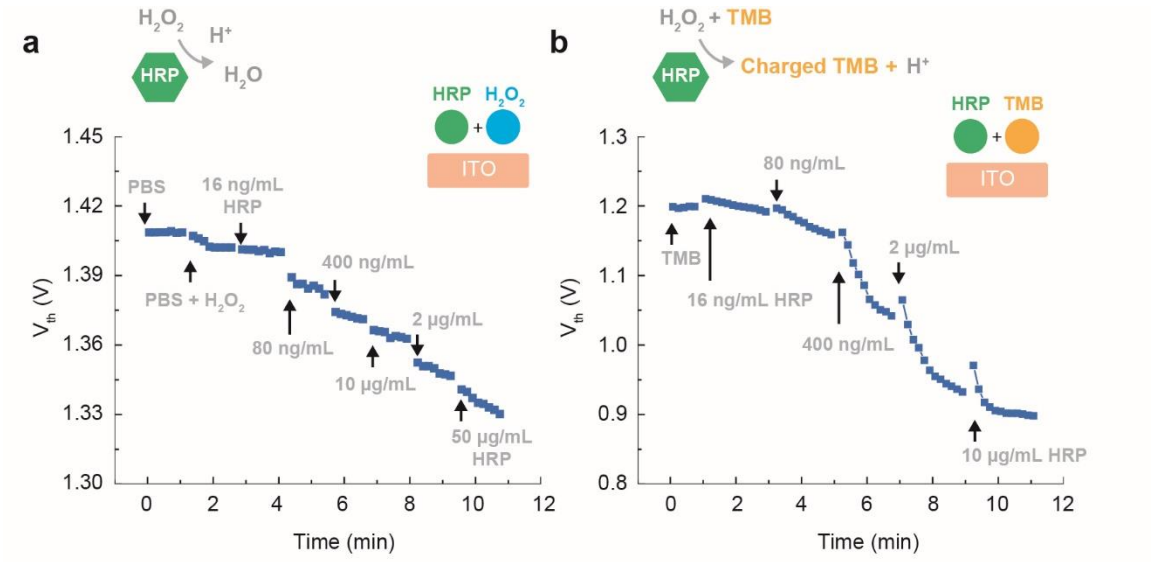

Figure S9. In the presence of HRP, hydroperoxide (H_2O_2) oxidizes TMB to the colored product.[1] Ab-HRP and H_2O_2 reaction was characterized in Figure S9a; Ab-HRP was not immobilized on the ITO surface but was free-floating in the solution with consistent concentrations of H_2O_2 and TMB over all solutions in Figure S9b. Initial V_{th}

in PBS without H_2O_2 and HRP was measured to be ca. 1.417 V (Figure 3a). V_{th} slightly decreased to ca. 1.4 V for PBS and H_2O_2 mixture (still without Ab-HRP) due to acidic properties of H_2O_2. V_{th} began to decrease when 80 ng/mL Ab-HRP was added to PBS and H_2O_2 mixture as Ab-HRP produced protons from H_2O_2. The results in Figure S7b also suggested that our detection system can translate Ab-HRP and TMB interactions. Pure TMB without Ab-HRP was initially acidic (pH of 4-5) which was estimated to be V_{th} of 1.2 V. No significant signal was observed from 16 ng/mL Ab-HRP in TMB, but V_{th} decreased with increasing Ab-HRP concentrations from 80 ng/mL to 10 µg/mL.

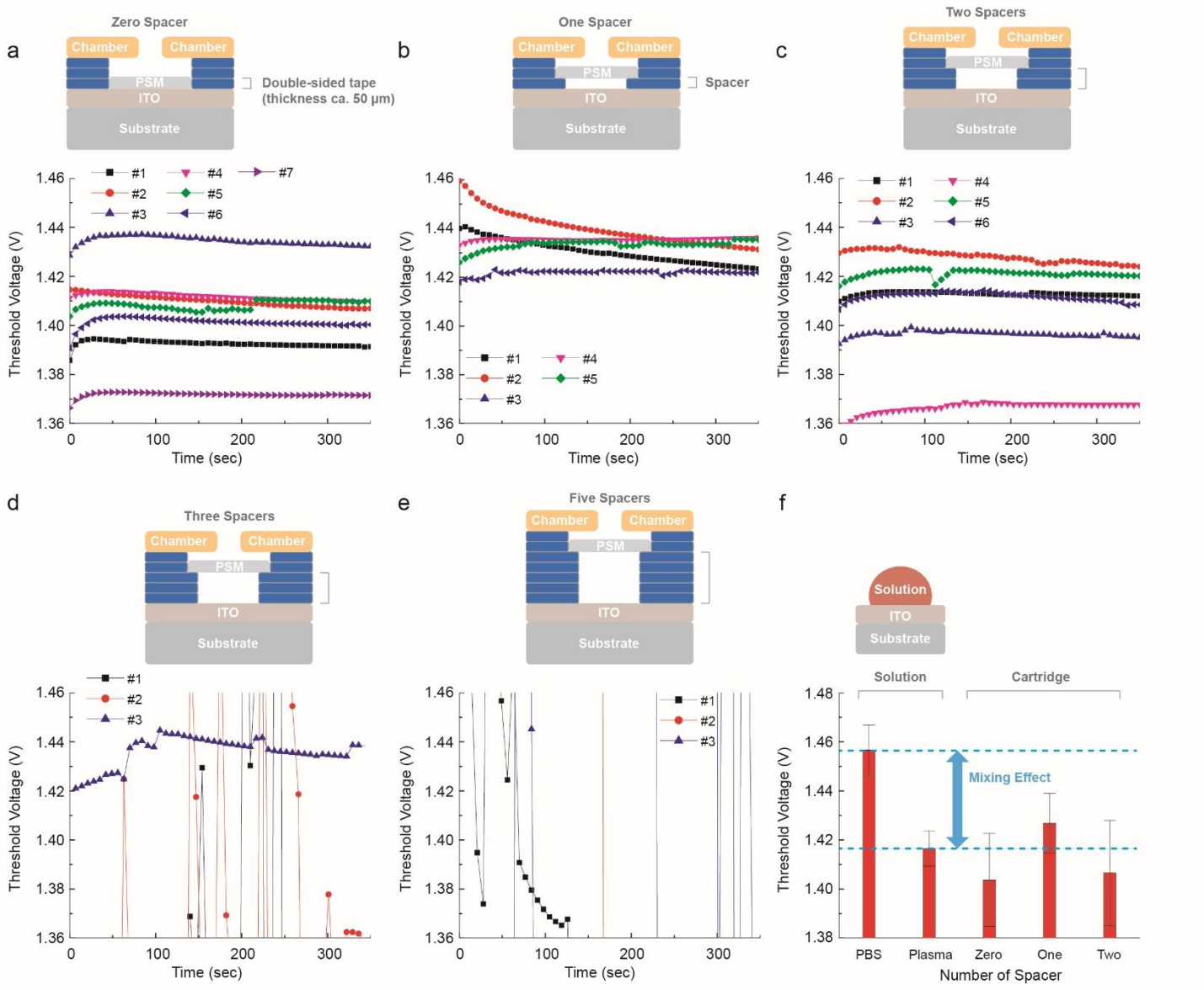

Figure S10. The V_{th} curves of cartridges with varying spacer configurations between the PSM and ITO: (a) zero, (b) one, (c) two, (d) three, and (e) five spacers. For each configuration, multiple cartridges were measured to ensure consistency: 7 cartridges for Figure S10a, 5 for Figure S10b, 6 for Figure S10c, and 3 each for Figures

S10d and S10e. All PSMs were fabricated using the method described in the Experimental section, employing the same batch throughout the study to maintain uniformity. Each cartridge was tested with a 20 µL volume of lipoprotein-free human plasma (Kalen Biomedical), allowing for a direct comparison of the effect of different air gaps on the sensor's electrical characteristics. The height of the air gap was controlled by the thickness of the double-sided tape used for mounting the ITO to the PSM. We opted for the thinnest commercially available double-sided tape, with a thickness of approximately 50 µm, to ensure precise control over the spacing. A detailed explanation of the cartridge structure and the method for controlling the space between the PSM and ITO is provided in the newly prepared Figure S10. The absence of an air gap led to significant variations in the baseline, as depicted in Figure S10a, due to the lack of space between the ITO and PSM, which restricts controllable mixing of plasma and buffer components (Figure S10a). Conversely, a 50 µm air gap, imposed by a spacer between the ITO and PSM, leads to a more controlled baseline (Figure S10b) compared to a cartridge without a spacer (Figure S10a). The average V_{th} of the cartridge with this air gap was approximately 1.426 V. Given that the V_{th} values observed for plasma and PBS buffer solution on the bare ITO were about 1.459 V and 1.419 V, respectively (Figure S10f), this setup demonstrates that effective mixing between the dried buffer components in the PSM and the plasma was achieved. In contrast, cartridges with two spacers (Figure S10c) began to exhibit divergent V_{th} ranges, similar to those observed with zero spacers (Figure S10a), because a larger air gap between the PSM and ITO results in poor solution contact on the ITO. Moreover, cartridges with three (Figure S10d) and five spacers (Figure S10e) did not produce a signal because the injected plasma could not bridge the gap between the reference electrode and the ITO; the air pocket formed below the PSM prevents the plasma from reaching the ITO electrode. Therefore, a spacer thickness of approximately 50 µm provides optimal mixing effects, which is why we used one spacer.

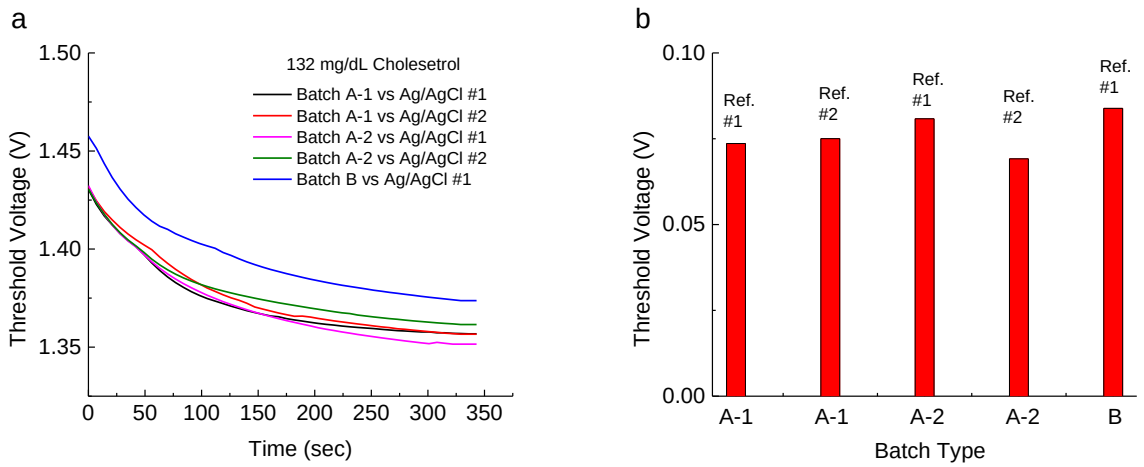

Figure S11. (a) V_{th} curves obtained from the same clinical plasma sample (132 mg/dL cholesterol), measured using cartridges from different batches and employing different Ag/AgCl reference electrodes. The potential effects of electrode contamination were assessed using data presented in Figure 2e. Figure S11a shows V_{th} curves from a cartridge, using identical clinical plasma samples measured at different times with the two Ag/AgCl reference electrodes. These measurements involved a cartridge prepared from the same batch but employed at distinct times, hence arbitrarily labeled as A-1 and A-2 to indicate the different measurement sessions. The performance of cartridges from batch A-1 was consistent, indicating negligible differences between electrodes #1 and #2. These electrodes were then used to assess 12 different clinical samples. Subsequently, the same 132 mg/dL plasma sample was measured again, now labeled as A-2, using a different reference electrode. Although slight variations were observed, the CV for ΔV_{th} remained within an acceptable range, approximately 5.58%, suggesting minimal contamination effects. Significantly, the primary source of variation in the V_{th} curves stemmed from batch differences, as observed in Batch B cartridges, even though the same 132 mg/dL plasma sample was used (Figure S11a). Variations in cartridge manufacturing across different batches often lead to disparate baseline ranges. Despite these differences in the starting points of the V_{th} curves depicted in Figure S11a, the ΔV_{th} was consistent (Figure S11b), showing an overall CV for ΔV_{th} of 6.84% across the identical plasma samples. This consistency underscores the robustness of our approach in maintaining accuracy despite variability in manufacturing and electrode use.

Reference

(1) Fanjul-Bolado, P.; Gonzalez-Garia, M. B.; Costa-Garcia, A. Amperometric detection in TMB/HRP-based assays. *Anal Bioanal Chem* **2005**, *382* (2), 297-302. DOI: 10.1007/s00216-005-3084-9.